Small molecules targeting histone H4 as potential therapeutics for chronic myelogenous leukemia

C. James Chou,[1] Michelle E. Farkas,[2] Sherry M. Tsai,[2] David Alvarez,[1] Peter B. Dervan,[2] and Joel M. Gottesfeld[1]

[1]Department of Molecular Biology, The Scripps Research Institute, La Jolla, California and [2]Division of Chemistry and Chemical Engineering, California Institute of Technology, Pasadena, California

Abstract

We recently identified a polyamide-chlorambucil conjugate, 1R-Chl, which alkylates and down-regulates transcription of the human histone *H4c* gene and inhibits the growth of several cancer cell lines *in vitro* and in a murine SW620 xenograft model, without apparent animal toxicity. In this study, we analyzed the effects of 1R-Chl in the chronic myelogenous leukemia cell line K562 and identified another polyamide conjugate, 6R-Chl, which targets H4 genes and elicits a similar cellular response. Other polyamide conjugates that do not target the *H4* gene do not elicit this response. In a murine model, both 1R-Chl and 6R-Chl were found to be highly effective in blocking K562 xenograft growth with high-dose tolerance. Unlike conventional and distamycin-based alkylators, little or no cytotoxicities and animal toxicities were observed in mg/kg dosage ranges. These results suggest that these polyamide alkylators may be a viable treatment alternative for chronic myelogenous leukemia. [Mol Cancer Ther 2008;7(4):769–78]

Introduction

Therapies targeting specific genes or gene products are a major aim of modern cancer biology and intervention (1–4). Notable recent successes in the field include both monoclonal antibodies (5, 6) and small molecules that target enzymes and receptors that are overexpressed or mutated in various cancers (3, 7, 8). Notwithstanding these important developments, DNA-alkylating agents remain the most common drugs for treatment of several solid and hematologic malignancies (9–11). Myelotoxicity and concomitant cytotoxicity due to limited DNA sequence selectivity is often the dose-limiting factor for use of these compounds in humans. Alkylating agents based on the minor groove binder distamycin A, including tallimustine and brostallicin, have shown improvements over nonconjugated DNA-alkylating agents in terms of affinity and specificity at the nucleotide level (12–15). However, these compounds possess only limited specificity (16), and myelotoxicity is still the dose-limiting factor in establishing an effective chemotherapy (12, 13).

Pyrrole-imidazole polyamides are a class of sequence-specific DNA-binding small molecules that have been shown to have high binding specificity and affinity, with some molecules even exceeding the binding affinities of transcription factors (17). Many polyamides are cell permeable and readily localize to the nuclei of cultured cells (18–21). Polyamides are effective inhibitors of RNA transcription when they disrupt essential protein-DNA interactions at promoter and enhancer elements (17, 22–25), and they may also modulate gene expression by modifying chromatin structure (26–28). Linked with DNA-alkylating agents, such as chlorambucil (29) or CC-1065/CBI derivatives (30, 31), polyamide conjugates react covalently with DNA at specific sites and inhibit transcription by stalling RNA polymerase during elongation.

Recently, α-diaminobutyric acid–linked hairpin polyamide-chlorambucil conjugates have been shown to bind and alkylate DNA sequences both *in vitro* and in cell culture models, with good sequence specificity (32–34). Initial screens of various hairpin polyamide-chlorambucil conjugates have shown the polyamide 1R-Chl (Fig. 1A, *top*) to be an inhibitor of cell proliferation in various cancer cell lines with no apparent cytotoxicity and little or no murine animal toxicity (32, 33, 35). This molecule binds within the coding region of the histone *H4c* gene both *in vitro* and in SW620 human colon carcinoma cells and down-regulates *H4c* transcription. Polyamides with similar pyrrole and imidazole compositions targeted to different DNA sequences failed to alkylate the coding region of the histone *H4c* gene and were found to be inactive both in cell culture and in a SW620 xenograft cancer model (32).

Studies suggest a two-hit mechanism for the observed cellular effects of 1R-Chl: down-regulation of histone gene transcription causes nucleosome depletion, followed by widespread alkylation of open chromatin, which elicits cell cycle arrest through the DNA repair pathway (35). Although our initial results point to the histone *H4c* gene

Received 2/4/08; accepted 2/22/08.

Grant support: National Cancer Institute grant CA107311 and Department of Defense grant CM043013 (J.M. Gottesfeld and P.B. Dervan) and predoctoral NIH National Research Service Award training grant (M.E. Farkas).

The costs of publication of this article were defrayed in part by the payment of page charges. This article must therefore be hereby marked *advertisement* in accordance with 18 U.S.C. Section 1734 solely to indicate this fact.

Note: Current address for D. Alvarez: New Jersey Center for Science, Technology and Math Education, Kean University, 1000 Morris Avenue, Townsend Hall 117-H, Union, NJ 07083-0411.

Requests for reprints: Peter B. Dervan, Division of Chemistry and Chemical Engineering, California Institute of Technology, Pasadena, CA 91125. E-mail: dervan@caltech.edu or Joel M. Gottesfeld, Department of Molecular Biology, The Scripps Research Institute, La Jolla, CA 92037. E-mail: joelg@scripps.edu

doi:10.1158/1535-7163.MCT-08-0130

A

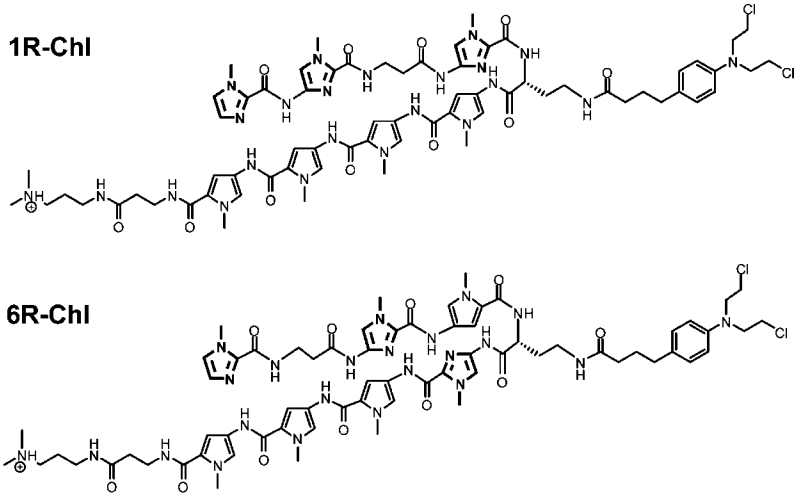

B

```
atgtctggtc gcggcaaagg cggaaaaggc ttggggaagg gtggtgctaa
gcgccatcgt aaggtgctcc gggataacat ccagggcatt acaaaaccgg
ctattcgccg tttggctcgg cgcggtggcg tcaagcgcat ttccggtctt
atctatgagg agactcgagg tgtgcttaag gttttcttag agaacgttat
tcgagacgcc gtcacctata cggagcacgc caagcgcaaa actgtcacag
ccatggatgt agtatatgcc ctaaaacgtc aggggcgcac tctgtatggc
ttcggcggct gaatctaaga atacgcggtc tcctgagaac ttcaaaaaac
aaaaacaaaa aaacccaaag gccctttca gggccgctca
```

Figure 1. DNA sequence of the coding region of the human histone *H4c* gene and chemical structures of 1R-Chl and 6R-Chl. **A,** chemical structures of 1R-Chl (*top*) and 6R-Chl (*bottom*), which target the DNA sequences 5′-WGGWGW-3′ and 5′-WGWGCW-3′, respectively (where W = A or T). *Bold,* imidazole rings. **B,** DNA sequence of the coding region of the human histone *H4c* gene. *Bold,* potential binding sites for 1R-Chl and 6R-Chl. Alkylation sites of 1R-Chl (*bold italic*) and 6R-Chl (*underlined*) as verified by LM-PCR.

as the major target of 1R-Chl, microarray studies in the SW620 cancer cell line indicate that the mRNA levels of several other genes are also affected (32). Thus, down-regulation of other genes may be involved in the cellular response to 1R-Chl.

In the present study, we extend our analysis to the well-established chronic myelogenous leukemia (CML) cell line K562. If histone H4 genes are the primary targets of 1R-Chl that lead to a block in cancer cell proliferation (35), other polyamide-chlorambucil conjugates targeting H4 genes would be predicted to elicit the same cellular response. We describe the synthesis and characterization of a small library of constitutional isomers of 1R-Chl. These molecules have the same chemical composition as 1R-Chl but would be expected to bind different DNA sequences. One conjugate, 6R-Chl (Fig. 1A, *bottom*), which targets sites adjacent to and overlapping the binding site for 1R-Chl (Fig. 1B) in the *H4c* gene, was found to have biological properties similar to 1R-Chl both in K562 cell culture and in a mouse xenograft model established with K562 cells. Other polyamide-chlorambucil alkylators that did not bind within the *H4c* gene or down-regulate histone H4 expression had no effect on cell proliferation. Microarray analysis in K562 cells reveals that the histone H4 genes *H4c* and *H4j/H4k* are down-regulated by 1R-Chl treatment. Transcripts for the *H4k* and *H4j* genes cannot be distinguished due to similarity in sequence. In addition, we explored the pharmacokinetic properties of 1R-Chl, the results of which point to this class of molecules as potential human cancer therapeutics.

Materials and Methods

Synthesis and Characterization of Pyrrole-Imidazole Polyamides

Pyrrole-imidazole polyamides were synthesized by standard solid-phase methods (36) using α-(*R*)-2,4-diaminobutyric acid or α-(*S*)-2,4-diaminobutyric acid as the hairpin turn unit (33). Polyamide-chlorambucil conjugates were generated as previously described (29), whereby the carboxylic acid of chlorambucil (Sigma-Aldrich) is activated and coupled to the free amine of the hairpin turn. The identity and purity of the compounds were established by mass spectrometry (MS) analysis (matrix-assisted laser desorption/ionization time-of-flight mass spectroscopy and electrospray mass spectroscopy) and analytic high-performance liquid chromatography, respectively.

Binding affinities of the parent polyamides (which lack chlorambucil) for target match and mismatch sites were determined by quantitative DNase I footprinting (37) using a radiolabeled DNA fragment of the plasmid pMFST6 (Supplementary Fig. S1A).[3] The plasmid was constructed by annealing the oligonucleotide pair 5′-AGCTGTAG-TATCTATAGTGCTTACTATCTATAGTCCTTACTATC-TATAGCTCTTACTATCTATAGCTGTTACTATCTATAC-TATCTAC-3′ and 5′-CATCATAGATATCACGAATGATA-GATATCAGGAATGATAGATATCGAGAATATAGA-TATCGACAATGATAGATAGATAGATGCTAG-3′.

[3] Supplementary material for this article is available at Molecular Cancer Therapeutics Online (http://mct.aacrjournals.org/).

Annealed oligonucleotides were ligated into the *Bam*HI/*Hin*dIII restriction fragment of pUC19 using T4 DNA ligase, and the plasmid was transformed into *Escherichia coli* JM109 competent cells. Ampicillin-resistant white colonies were selected from 25 mL Luria-Bertani agar plates containing 50 mg/mL ampicillin treated with 5-bromo-4-chloro-3-indolyl-β-D-galactopyranoside and isopropyl-L-thio-B-D-galactopyranoside solutions and grown overnight at 37°C. Cells were harvested the following day, and purification of the plasmid was done with a Wizard Plus Midiprep DNA Purification kit (Promega). Alkylation experiments done on the pMFST6 insert were done as previously described (29). Alkylation experiments were also done on a 240-bp region of the *H4c* mRNA coding sequence, which was amplified from genomic DNA with the following PCR primers: 5′-GTGCTAAGCGCCATCGTAAG-3′ and 5′-CCCTGACGTTTTAGGGCATA-3′. These experiments were conducted using 10 ng of the PCR product incubated for 16 h at 37°C in 100 μL of 20 mmol/L NaCl and 10 mmol/L Tris-Cl (pH 7.4), with each of the polyamide-chlorambucil conjugates at 10, 100, and 1,000 nmol/L concentration followed by thermal cleavage and primer extension labeling, as described (32).

Cell Lines and Cell Viability Assays

The human CML lymphoblast cell line K562 (purchased from the American Type Culture Collection), which contains the b3a2 Bcr-Abl translocation, was used in this study. Cells were grown and maintained in RPMI 1640 containing 10% fetal bovine serum under standard mammalian cell culture conditions as recommended by the American Type Culture Collection. Direct phase-contrast microscopic visualization was used to monitor the effects of polyamide-chlorambucil conjugates on cell growth rates and cell morphology. Promega CellTiter 96 Aqueous One Solution Cell Proliferation assay [using 3-(4,5-dimethylthiazol-2-yl)-5-(3-carboxymethoxyphenyl)-2-(4-sulfophenyl)-2H tetrazolium (MTS) conversion to formazan to examine mitochondrial activity], trypan blue exclusion (Vi-Cell XR viability analyzer, Beckman Coulter), and Annexin V-FITC/propidium iodide apoptosis staining (BD PharMingen) were used to determine cell proliferation (EC_{50}), viability, and initiation of apoptosis, respectively.

Cell Cycle Analysis

The effects of polyamide-chlorambucil conjugates on cell cycle progression were monitored by flow cytometry analysis in the Scripps fluorescence-activated cell sorting core facility. Polyamide-treated cells (250 nmol/L of polyamide in culture medium for 24 h) were collected by centrifugation (200 × *g* for 5 min). Cell pellets were resuspended in 500 μL PBS and fixed with addition of 4.5 mL of prechilled 70% ethanol, stained with propidium iodide (50 μg/mL), and analyzed for DNA content, reflecting the fraction of cells at each point in the cell cycle (G_0-G_1, S, and G_2-M). Cells with less than a 2C DNA content are indicative of DNA fragmentation and apoptosis.

Ligation-Mediated PCR

K562 CML cells were incubated in culture medium for 24 h with each of the polyamide-chlorambucil conjugates at a 250 nmol/L concentration followed by digestion of purified DNA with *Dra*I, thermal cleavage, and ligation-mediated PCR (LM-PCR) using the primers for the *H4c* gene listed above, as previously described (32).

Real-time Quantitative Reverse Transcription-PCR

RNA from polyamide-treated cells was extracted using the Absolutely RNA Miniprep kit (Stratagene). Reverse transcription-PCR (RT-PCR) was done using iScript One-Step RT-PCR kit with SYBR Green (Bio-Rad Laboratories) in accordance with the manufacturer's instructions. Levels of *H4c*, *H4k/H4j*, *SMG1*, *RPL13*, *HNRPD*, *RAB35*, and *H2AFY* transcripts were quantified by amplifying a segment of their respective mRNAs with appropriate primer sets (Supplementary Table S1). The reverse transcription reaction was carried out at 50°C for 10 min followed by iTaq hot-start DNA polymerase activation by heating at 95°C for 15 min. Three-step cycling was done: denaturation of 15 s at 95°C, annealing of 30 s at 55°C, and extension of 30 s at 72°C for 45 cycles. All gene expression levels were normalized by parallel amplification and quantification of mRNA levels for the housekeeping gene glyceraldehyde-3-phosphate dehydrogenase mRNA as an endogenous reference with the following primers: 5′-GAGTCAACGGATTTGGTCGT-3′ and 5′-GAGGTCAATGAGGGGTCAT-3′.

SDS-PAGE and Western Blot Analysis

Equal numbers of cells were lysed with radioimmunoprecipitation assay buffer [50 mmol/L Tris-HCl (pH 7.4), 1% NP40, 0.25% deoxycholate, 1 mmol/L EDTA] with 1× complete mini protease inhibitor cocktail (Roche Diagnostics) for 30 min at 4°C followed by 15-s sonication pulses (Branson Sonifier 150 at 3 W). Cell lysates were then centrifuged at 14,000 rpm (12,000 × *g*) for 15 min and the supernatants were removed and combined with lithium dodecyl sulfate sample loading buffer (Invitrogen). SDS-PAGE was done with the Invitrogen NuPAGE system using 4% to 12% Bis-Tris gels and MES running buffer (Invitrogen). Electrophoresis was carried out at 200 V for 45 min, and gel contents were transferred at 30 V for 1 h to a 0.2 μm nitrocellulose membrane. Membranes were then blocked with 5% bovine serum albumin for 1 h at 4°C and probed with histone H4 or glyceraldehyde-3-phosphate dehydrogenase (Abcam) primary antibodies. Protein-antibody complexes were then visualized by enhanced chemiluminescence using Amersham ECL system (GE Healthcare) with either anti-rabbit or anti-goat horseradish peroxidase–conjugated secondary antibodies (Santa Cruz Biotechnology).

Xenograft Studies of 1R-Chl, 6R-Chl, and 1S-Chl

Female athymic nude mice were purchased from The Scripps Research Institute Division of Animal Resources. Experimental protocols were approved by the Scripps Institutional Animal Welfare Committee. K562 cells were suspended to 50 million cells/mL in Matrigel (BD Biosciences), 0.2 mL of which was s.c. injected into the rear left flank of each mouse (6–8 wk of age). Mice were monitored and tumor sizes were measured daily; tumor volumes were

calculated as 0.5 × length × (width)^2. Tumors were staged for 7 to 14 d to enter growth phase. At this point, compounds were given at a dose of 7.5 mg/kg per injection via the tail vein thrice over a 5-d period.

Pharmacokinetic Properties of 1R-Chl and 1S-Chl

Pharmacokinetic studies were done in normal BALB/c mice to determine plasma levels of the compounds 1R-Chl and 1S-Chl over time and to calculate their constant of elimination (k_{el}), half-life ($t_{1/2}$), and volume of distribution (V_d). Forty-eight female BALB/c mice were divided into three groups of 16 mice each. Group 1 received 100 μL (100 nmol) of 1 mmol/L 1R-Chl, group 2 received the same amount of 1S-Chl, and group 3 received an equal volume of PBS (control) via i.v. bolus injection. Blood (0.5 mL) was collected from each animal at specific time points (0, 5, 15, and 30 min and 1, 4, 8, and 24 h) in heparinized tubes, then allowed to coagulate at ambient temperature for 24 h, and centrifuged at 3,100 rpm for 10 min to separate the serum from the clot.

Concentrations of 1R-Chl and 1S-Chl in the serum were determined by MS (see below). Each time point had two animals per group. Data collected were plotted as concentration (Y axis) versus time (X axis) and subjected to first-order kinetic analysis to calculate the pharmacokinetic variables. From this graph, $t_{1/2}$ was calculated, and from the natural logarithm of the concentration versus time, k_{el} (slope) and V_d (dose/anti-logarithm Y-intercept) were determined (Y-intercept represents the theoretical concentration at $t = 0$). V_d for humans was predicted by multiplying the V_d by 70 kg (average human weight).

1R-Chl distribution in the mouse body was analyzed as follows: mice were injected with 500 nmol of 1R-Chl or PBS and euthanized after either 2 or 24 h; organs were fixed in formalin. A small piece from each major organ was weighed, homogenized in PBS buffer, and sonicated by two pulses of 15 s each. 1R-Chl concentration was determined by MS (see below).

MS Determination of 1R-Chl and 1S-Chl

A control polyamide-chlorambucil conjugate, with the sequence ImImPyIm-$(R)^{Chl}$γ-PyPyPyPy-β-Dp, was used as an internal standard for concentration determination by MS. The molecular mass of this molecule differs from 1R-Chl and 1S-Chl by 79.1 a.m.u. From each sample, a 200 μL serum aliquot was taken to which 2 μL of 100 pmol/μL control polyamide solution were added along with 800 μL of chilled 100% methanol. Samples were vigorously vortexed for 1 min and then incubated for 15 min at 4°C. They were subsequently centrifuged at 12,000 rpm for 10 min, and the supernatant was harvested and concentrated to 50 μL by methanol extraction. Standards with concentrations from 100 to 12,500 fmol/μL of 1R-Chl or 1S-Chl were prepared in serum and extracted by the above procedure. Concentrations were determined by electrospray MS with an Agilent 1100 single quadrupole instrument coupled to an Agilent 1100 liquid chromatography system and a 50 mm × 2.0 mm C18 column for injection and separation.

Results

Only Polyamides Targeting Histone H4 Genes Are Potent Inhibitors of K562 Cell Proliferation

To investigate the effects of pyrrole-imidazole polyamide-chlorambucil conjugates on K562 cells, we synthesized a small library of constitutional isomers of 1R-Chl, along with its stereoisomer, 1S-Chl (Fig. 2A). All molecules targeted the general DNA sequence 5′-WGNNNW-3′ (where W = A or T; N = A, C, G, or T); the binding site for 1R-Chl is 5′-WGGWGW-3′. Binding affinities for nonalkylating parent molecules were determined via quantitative DNase I footprinting on plasmid inserts containing match sites (Fig. 2A). It has been previously shown that attachment of the chlorambucil moiety does not seem to affect DNA-binding properties (29). Affinities for 1R, 3R, 5R, and 1S have been previously reported (33–35); polyamides 4R and 6R were analyzed on plasmid insert pMFST6 (Supplementary Fig. S1B). All polyamides were found to bind their expected match sites.

The ability of each polyamide-chlorambucil conjugate to alkylate nucleotides adjacent to its match binding sites on synthetic DNA constructs was also evaluated. Alkylation profiles of polyamides 1R-Chl, 3R-Chl, 5R-Chl, and 1S-Chl have been previously reported (33–35); polyamides 4R-Chl and 6R-Chl were analyzed on plasmid insert pMFST6 (Supplementary Fig. S1C). All polyamides alkylated DNA in the nanomolar concentration range. *H4c* gene-specific DNA alkylation activities were monitored with the polyamide-chlorambucil conjugates on a PCR product derived from the *H4c* gene. Significantly, only 1R-Chl and 6R-Chl have binding sites within the *H4c* gene and only these compounds effectively alkylate the *H4c* PCR product *in vitro* (Supplementary Fig. S2). 6R-Chl targets the DNA sequence 5′-WGWGCW-3′; the sequence 5′-TGTGCT-3′ is found both adjacent to and overlapping the binding site for 1R-Chl on the top strand of the *H4c* and *H4k/H4j* genes (5′-AGGTGT-3′; Fig. 1B).

Polyamide-chlorambucil DNA alkylators were then tested for effects on growth and morphology of K562 cells. Only cells treated with either 1R-Chl or 6R-Chl exhibited growth inhibition at 250 nmol/L; all others were inactive against K562 proliferation at the same concentration. The control polyamide 5R-Chl has EC_{50} of 4.2 μmol/L, and 3R-Chl, 4R-Chl, and 1S-Chl have EC_{50}s of >10 μmol/L (Fig. 2A and B; Supplementary Fig. S3). This reflects a minimum 16-fold difference in EC_{50} values for the active polyamide conjugates relative to the controls. 1R-Chl and 6R-Chl also caused an enlargement of cell volume at 250 nmol/L and induced G_2-M cell cycle arrest (Fig. 2C and D). Following treatment with 1R-Chl or 6R-Chl for 3 to 6 days, an increase in the number of apoptotic cells was observed via Annexin V-FITC/propidium iodide fluorescence-activated cell sorting analysis (Fig. 2D). Other polyamide-chlorambucil conjugates had no effect on apoptosis (Supplementary Fig. S4).

Alkylation of the H4 Genes by 1R-Chl and 6R-Chl in K562 Cells

LM-PCR (38) was used to determine sites of alkylation by 1R-Chl and 6R-Chl on the *H4c* gene in K562 cells.

A

Polyamide	Sequence	Match Site (Plasmid)	Ka Match Site (M^{-1}) X = NH^{3+}	Growth Arrest EC50 (M) X = Chl	Cell Enlargement
1R	5'-WGGWGW-3'	5'-TAGGTGT-3' (pMFST2)	$6.7(\pm 0.1) \times 10^{9}$	$3.0(\pm 1.5) \times 10^{-7}$	yes
3R	5'-WGGWCW-3'	5'-TAGGTCT-3' (pJG)	$7.4(\pm 0.6) \times 10^{8}$	$> 1 \times 10^{-5}$	no
4R	5'-WGCWGW-3'	5'-AAGCTGT-3' (pMFST6)	$1.1(\pm 0.3) \times 10^{8}$	$> 1 \times 10^{-5}$	no
5R	5'-WGWGGW-3'	5'-TAGTGGT-3' (pMFST)	$8.0(\pm 0.6) \times 10^{8}$	$4.2(\pm 0.5) \times 10^{-6}$	no
6R	5'-WGWGCW-3'	5'-TAGTGCT-3' (pMFST6)	$4.9(\pm 0.5) \times 10^{9}$	$8.1(\pm 2.4) \times 10^{-8}$	yes
1S	5'-WGWGGW-3'	5'-TAGGTGT-3' (pMFST2)	$4.8(\pm 0.9) \times 10^{8}$	$> 1 \times 10^{-5}$	no

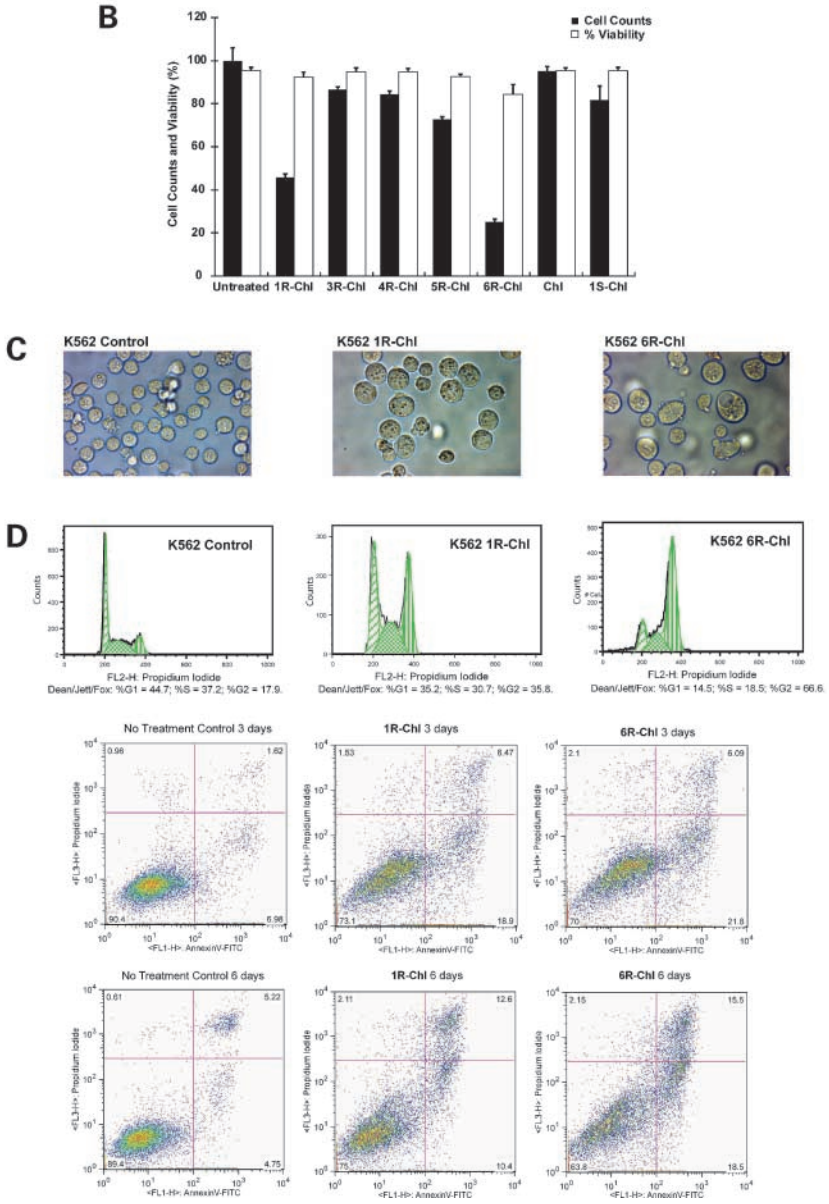

Figure 2. Analysis of a polyamide library. **A,** shown in the table are the following: ball-and-stick model for the structure of each polyamide (*closed circles*, imidazoles; *open circles*, pyrroles; *diamonds*, β-alanines; *semicircle with positive sign*, dimethylaminopropylamine; *X*, a free amino group in the parent polyamide or chlorambucil in the conjugates); targeted match binding sites for the polyamides, where W = A or T (names of plasmid constructs on which footprinting and alkylation assays were done are shown in parentheses); equilibrium association constants of the parent polyamides as determined by quantitative DNase I footprinting (SDs are in parentheses); the effective concentration 50 (EC_{50}) against K562 cell proliferation was determined by MTS assay (SDs are in parentheses); effects of polyamide-chlorambucil conjugates on cell morphology (enlargement) and growth. **B,** effect of polyamides on growth and viability of K562 cells. Cells were incubated with the indicated polyamides at 250 nmol/L for 3 d. Only 1R-Chl and 6R-Chl affected cell proliferation. **C,** phase microscopy images illustrate that 1R-Chl and 6R-Chl induce an increase in cell volume at 250 nmol/L after 3 d. Treatments with all other polyamide conjugates and chlorambucil seem similar to control and do not show similar cell enlargement (Supplementary Fig. S4A). **D,** *top,* G_2-M cell cycle arrest is observed for 1R-Chl and 6R-Chl after 24 h of treatment with 250 nmol/L polyamide. 6R-Chl caused a greater G_2-M cycle arrest than 1R-Chl; all other polyamide-treated cells are similar to control and do not show any significant cycle perturbation (Supplementary Fig. S4B). Annexin V/propidium iodide staining of 1R-Chl – treated and 6R-Chl – treated cells after 3 and 6 d. Treatment of cells with 250 nmol/L 1R-Chl or 6R-Chl resulted in increased Annexin V – positive and propidium iodide – negative populations and Annexin V – positive and propidium iodide – positive populations. Treatments with other polyamide conjugates are similar to control and do not result in an effect (Supplementary Fig. S4C).

Cells were incubated with each of the hairpin polyamide-chlorambucil conjugates for 24 h at a concentration shown to cause growth arrest with 1R-Chl and 6R-Chl (250 nmol/L). After purification of genomic DNA and digestion with the restriction enzyme *Dra*I, the DNA was heated to induce strand breakage at sites of alkylation (29). LM-PCR with *H4c* gene-specific primers showed that both 1R-Chl and 6R-Chl alkylate the *H4c* gene in cultured K562

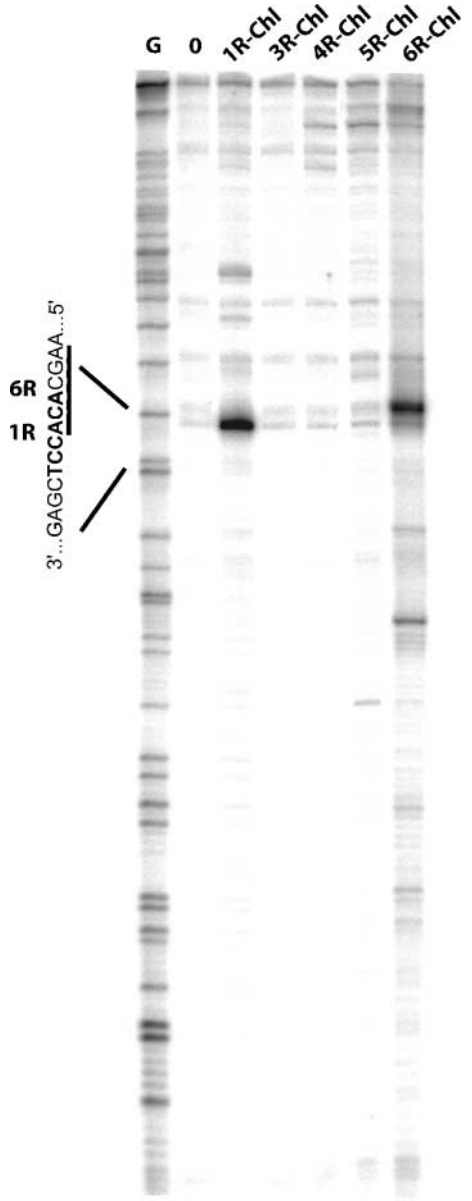

Figure 3. Alkylation of the *H4c* gene in K562 cells. Cells were incubated with the indicated polyamide-chlorambucil conjugates for 24 h followed by DNA purification and LM-PCR. The radiolabeled primer interrogates alkylation events on the bottom, coding strand of DNA. *0,* no polyamide control; *G,* guanine-only sequencing reaction done on a PCR product from the *H4c* gene followed by LM-PCR. *Left,* binding sites for 1R-Chl (*bold*) and 6R-Chl (*underlined*). Both molecules alkylate the adenine at the 5′ end of their respective binding site. Nonspecific background bands appear in all lanes and are unrelated to the polyamides.

cells. Consistent with *in vitro* alkylation results, other molecules in the library failed to alkylate the *H4c* gene in cell culture (Fig. 3).

RT-PCR and Western Blot Analyses of 1R-Chl in K562 Cells

Quantitative real-time PCR was used to verify the results of expression arrays for several significant genes from K562 microarray studies (Gene Expression Omnibus accession number GSE8832). The expression of histone H4 mRNAs *H4c* and *H4k/H4j* were decreased >60% compared with untreated control cells (Fig. 4A). Identical DNA-binding and alkylation sites for 1R-Chl are present in the *H4c, H4k*, and *H4j* genes. Western blot analysis for total histone H4 protein in whole-cell lysate shows significant down-regulation of total H4 protein levels after 24 h of incubation with 1R-Chl (Fig. 4B). Surprisingly, several of the most down-regulated and highly significant genes, based on *P* values and extent of down-regulation in microarray analysis (i.e., *SMG1, RPL13, HNRPD, RAB35,* and *H2AFY*), seemed not to be significantly affected by 1R-Chl when analyzed by real-time quantitative RT-PCR (qRT-PCR; Supplementary Fig. S5).

1R-Chl and 6R-Chl Arrest the Growth of K562 Xenografts

K562 cells were injected into athymic nude mice, and tumors were staged to >100 mm^3 (approximately 7–14 days after injection of cells). In a first experiment, mice

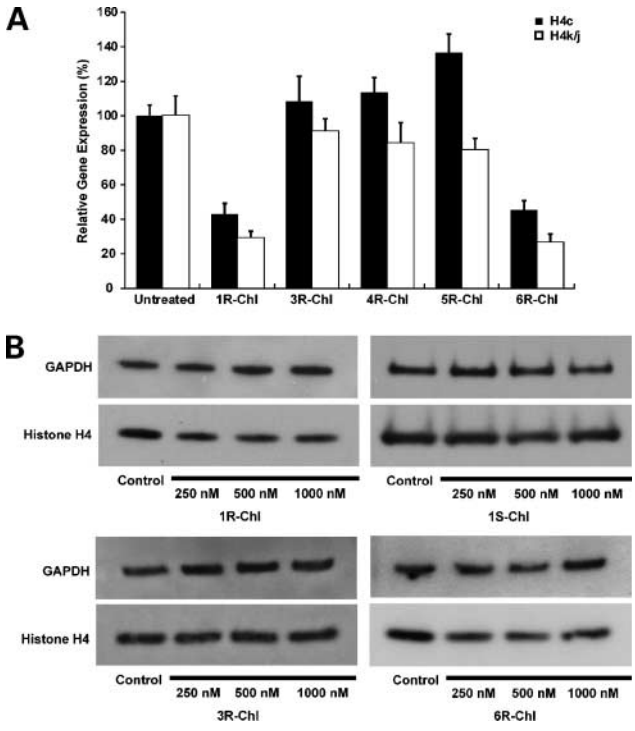

Figure 4. Effect of polyamides on histone *H4c* and *H4k/H4j* transcript expression and Western blot analysis. **A,** chart showing polyamide effect on *H4c* and *H4k/H4j* expression; only 1R-Chl and 6R-Chl caused gene down-regulation. **B,** K562 cells were treated with 1R-Chl (*top left*) and 6R-Chl (*bottom right*) at the indicated concentrations for 24 h, and histone H4 and glyceraldehyde-3-phosphate dehydrogenase (*GAPDH*) protein levels were assayed by Western blot analysis. After incubating with the secondary antibody, the membrane was washed thrice and soaked in enhanced chemiluminescence Western blotting reagents for 30 s. The membrane was visualized by autoradiography films after 5 to 30 s of exposure (5 s for H4 and 30 s for glyceraldehyde-3-phosphate dehydrogenase). Analysis of treatment with 1S-Chl (*top right*) and 3R-Chl (*bottom left*) did not show significant decreases in histone H4 levels.

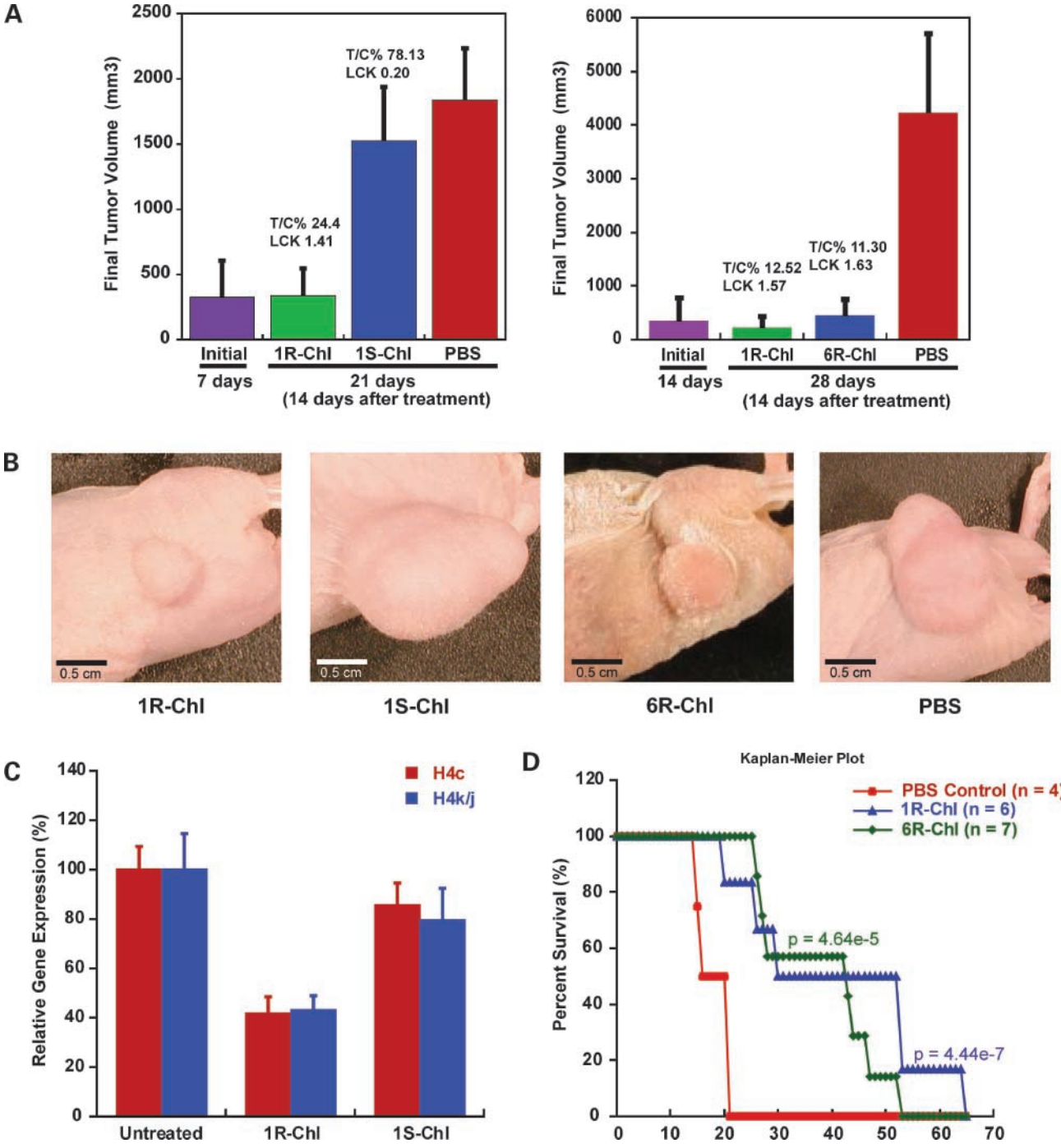

Figure 5. Murine K562 xenograft studies. **A,** athymic nude mice were injected with K562 cells and tumors were allowed to develop for either 7 d (*left*) or 14 d (*right*), after which mice were treated with the indicated polyamides; tumor volumes were determined 14 d later. **B,** representative photographs of 1R-Chl – treated, 6R-Chl – treated, 1S-Chl – treated, and PBS-treated animals. **C,** mRNA was isolated from tumor xenografts after treatment with 1R-Chl and 1S-Chl 24 h after the last injection. Real-time qRT-PCR showed down-regulation of *H4c* and *H4k/H4j* transcripts *in vivo* by 1R-Chl; 1S-Chl did not significantly down-regulate either *H4c* or *H4k/H4j*. **D,** Kaplan-Meier survival plot showing extended life span of 1R-Chl – treated and 6R-Chl – treated mice. The life extensions by both 1R-Chl and 6R-Chl are ~2 wk with $P = 4.44 \times 10^{-7}$ and 4.64×10^{-5}, respectively.

were i.v. injected with three doses of 1R-Chl, 1S-Chl, or PBS vehicle control (Fig. 5A, *left*); for a second experiment, mice were injected with 1R-Chl, 6R-Chl, or PBS vehicle (Fig. 5A, *right*). The molecule 1S-Chl was used as a control polyamide; although it targets the same sequence as 1R-Chl, the opposite stereochemistry of its turn unit results in a greatly reduced ability to bind and alkylate DNA (32, 33). The dosage routine was 7.5 mg/kg per injection and the

polyamides were given on treatment days 0, 2, and 5. The treatment dose of 1R-Chl was determined based on the LD_{20} of tallimustine and brostallicin, both of which have shown severe dose-limiting toxicities in the murine model and during phase II clinical trials (9, 39).

Mice treated with 1R-Chl and 6R-Chl showed immediate growth regression of the tumor xenografts, whereas 1S-Chl and PBS vehicle had no effect on tumor growth (Fig. 5A and B). Importantly, all mice treated with either 1R-Chl or 6R-Chl appeared healthy with minimal weight loss, whereas all mice treated with 1S-Chl and PBS vehicle showed signs of wasting with significant weight loss due to exponential tumor growth. No obvious toxicity was associated with polyamide treatment. Based on the T/C% (tumor volume analysis) and log cell kill (LCK) values (tumor growth delay), 1R-Chl and 6R-Chl treatments are highly effective: according to the National Cancer Institute standards, T/C < 42% and LCK > 0.7 are minimal levels for activity (39). For the two experiments conducted, the T/C% for 1R-Chl–treated mice versus untreated control were 24.4% and 12.52%, and LCK was 1.41 and 1.57, respectively. For 6R-Chl, the T/C% was 11.30% and LCK was 1.63. In contrast, treatment with 1S-Chl gives results outside of the therapeutic range (T/C% = 78.13 and LCK = 0.20).

Twenty-four hours following the final 1R-Chl treatment, K562 xenograft tumors were dissected and their mRNA was isolated for qRT-PCR analysis. Both *H4c* and *H4k/H4j* transcripts were observed to be down-regulated in tumors from 1R-Chl–treated mice. Analysis of tumor samples from 1S-Chl–treated and PBS-treated mice revealed no effect on histone *H4c/H4k/H4j* mRNA levels (Fig. 5C), consistent with *in vitro* results.

A Kaplan-Meier survival plot for mice treated with 1R-Chl or 6R-Chl versus PBS shows a significant extension in life span even after only one dosing regimen (Fig. 5D). We expect that prolonged administration of these polyamide-chlorambucil conjugates would extend life span even further and will be determined in future studies.

Pharmacokinetic Variables and Pharmacotoxicity of 1R-Chl

To predict the behavior and likely dosage regimen of the polyamides in humans, pharmacokinetic variables for 1R-Chl and 1S-Chl were determined in BALB/c mice. MS was used to determine polyamide concentration in serum following injection of 1R-Chl or 1S-Chl. Both compounds seemed to exhibit first-order decay kinetics after a brief lag time (Fig. 6A), indicating that the rate of elimination from serum is proportional to the concentration of the compound in serum at a particular time point. From these results, we determined that both 1R-Chl and 1S-Chl have $t_{1/2}$ values of ~2 h. k_{el} was determined by plotting the natural logarithm of 1R-Chl serum concentration versus time (during the clearance phase) and calculating the slope of the best-fit straight line; k_{el} was found to be ~0.45 h^{-1}. The concentration of the compound achieved in blood at $t = 0$ was determined by extrapolating the line to the *Y*-intercept. V_d was calculated by dividing the dose injected by this theoretical initial concentration (t_0). 1R-Chl was predicted to have a V_d of ~0.48 L/kg, corresponding to ~33.8 L for a 70 kg human (Fig. 6B). Pharmacokinetic variables for 1S-Chl were also determined and are similar to those of 1R-Chl: k_{el} of ~0.55 h^{-1}; V_d of ~0.68 L/kg; V_d of ~47.62 for a 70 kg human.

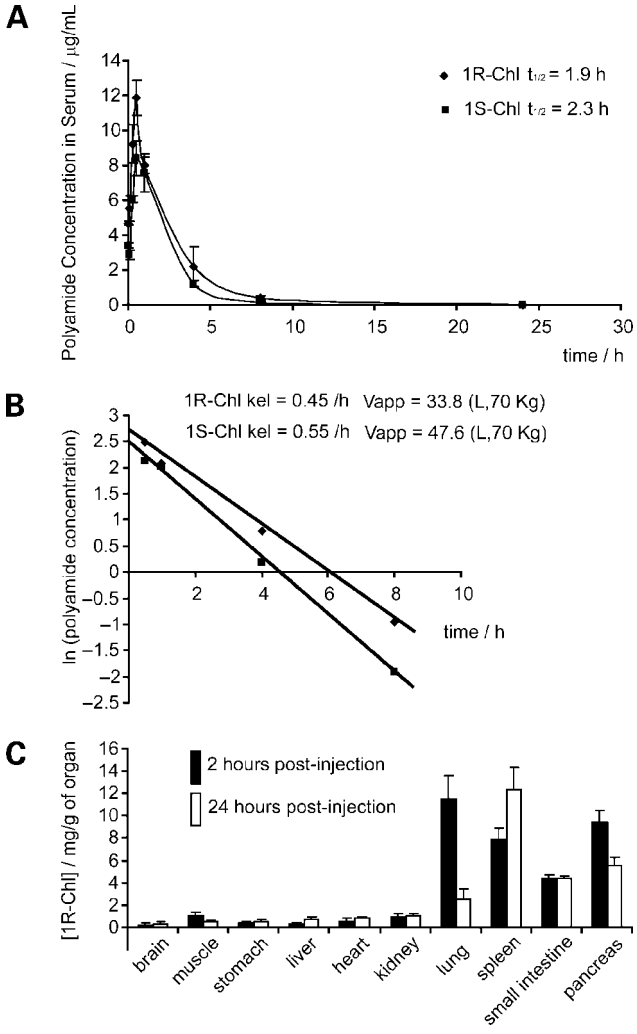

Figure 6. Pharmacokinetic variables and biodistribution of 1R-Chl. **A,** concentration (in μg/mL; *Y axis*) of 1R-Chl (*rhombus*) and 1S-Chl (*squares*) in serum over time. Mice were injected with either 1R-Chl or 1S-Chl (100 nmol, equivalent to 7.5 mg/kg) and blood was extracted at indicated time points. Amounts of polyamide were determined by MS, and $t_{1/2}$s for 1R-Chl and 1S-Chl were calculated. **B,** graph depicting the natural logarithm (*ln*) of 1R-Chl (*rhombus*) and 1S-Chl (*squares*) concentration versus time. *Y-intercept,* theoretical concentration at $t = 0$, where k_{el} and the apparent V_d were calculated. **C,** graph depicting the biodistribution of 1R-Chl. Mice were treated with 1R-Chl (500 nmol = 37.5 mg/kg) and euthanized either 2 h (*black columns*) or 24 h (*white columns*) after injection. Major organs were harvested, and a weighed portion of each was homogenized and sonicated. 1R-Chl concentration was determined by MS.

The distribution of 1R-Chl in various mouse organs was determined by MS (Fig. 6C). Following a 500 nmol dose, equal amounts of 1R-Chl were detected in the brain, muscle, stomach, liver, heart, and kidney; it is likely that

1R-Chl crosses the blood-brain barrier. Extensive amounts of 1R-Chl were found in the lung, spleen, small intestine, and pancreas after 2 h after injection and at $t_{1/2}$, as well as 24 h after injection, at which point 1R-Chl is undetectable in serum (Fig. 6A). These results indicate that 1R-Chl can be readily eliminated from serum and persist in peripheral organs after tissue entry.

Discussion

Histone Genes as Primary Targets of Polyamide-Chlorambucil Conjugates Leading to Growth Inhibition of Cancer Cells

In the library of polyamide-chlorambucil conjugates described herein, 1R-Chl and 6R-Chl are the only molecules expected to bind and alkylate within histone *H4c/H4k/H4j* genes. Sites of alkylation within the *H4c* gene are on the template strand, at the 5′ ends of the 1R-Chl and 6R-Chl targeted sequences (Figs. 1 and 3; Supplementary Fig. S2). Alkylation of this strand would be predicted to block transcription elongation by RNA polymerase II. Reporter gene assays have shown that alkylation of the template strand produces a more pronounced effect on transcription inhibition than on the noncoding strand (40). Real-time qRT-PCR and Western blot analyses confirm that K562 cells treated with 1R-Chl or 6R-Chl (250 nmol/L for 24 h) exhibit down-regulation of *H4c* and *H4k/H4j* transcripts and total histone H4 protein levels. Other polyamide-chlorambucil conjugates do not alkylate H4 genes *in vitro* or in living cells and neither affect *H4c* and *H4k/H4j* mRNA and histone H4 levels nor inhibit K562 cell growth.

Previous studies involving 1R-Chl have shown that down-regulation of the *H4c* gene in SW620 cells is required for growth inhibition, but changes in *H4k/H4j* transcription were not observed (32). Further inspection of Affymetrix microarray data for SW620 cells revealed that *H4k/H4j* genes are not highly expressed in SW620 cells relative to *H4c*. However, K562 cells have similar *H4c* and *H4k/H4j* expression levels as confirmed by real-time qRT-PCR. The primary targets of down-regulation by 1R-Chl in K562 cells were the histone H4 genes *H4c* and *H4j/H4k*. The only gene down-regulated by 1R-Chl in both K562 and SW620 cells is *H4c*, indicating it to be the key target that elicits growth effects. Furthermore, only cultured cell lines that express the histone *H4c* gene at high levels are affected by 1R-Chl (32, 35).

Polyamide-Chlorambucil Conjugates Block Tumor Progression with Little Animal Toxicity

Polyamides 1R-Chl and 6R-Chl are the first sequence-specific DNA alkylators reported to show little animal toxicity at mid to high mg/kg range with three consecutive injections every other day over 5 days. This dosing regimen is highly effective in blocking the growth of established tumors (Fig. 5). No behavior or significant weight changes were observed during experiments with normal BALB/c or xenograft mice. In comparison, tallimustine and brostallicin, both of which are micromolar DNA alkylators targeting AT-rich sequences, have shown significant animal toxicity at 4 and 0.8 mg/kg, respectively (9, 39).

We have shown here that 1R-Chl possesses desirable pharmacokinetic variables: it has a $t_{1/2}$ of $\sim$2 h, enough time to allow the drug to effectively reach its target while minimizing prolonged presence in the bloodstream, which can result in toxic effects. k_{el} of 1R-Chl is relatively low ($\sim 0.45\ h^{-1}$) compared with those of most anticancer drugs, indicating that, should a steady concentration of the drug be necessary to achieve efficacy, a regimen of constant infusion may be considered. The k_{el} of 1R-Chl is similar to that of capecitabine ($0.5\ h^{-1}$), a nonalkylating anticancer drug used to treat breast cancer. In addition, $V_d > 30$ for 1R-Chl, indicating that it is very well distributed in the body, an observation that is consistent with the presence of the molecule in the brain, muscle, stomach, liver, heart, and kidney in our biodistribution analysis (Fig. 6C). The pharmacokinetic variables for 1R-Chl are close to those of some commonly used chemotherapeutic drugs, including both alkylating agents and other types of compounds.

Polyamide-Chlorambucil Conjugates as Potential Therapeutics for CML and Other Forms of Cancer

The development of the selective p210 Bcr-Abl tyrosine kinase inhibitor Gleevec (STI 571, imatinib mesylate; Novartis) as a directed therapeutic for CML has been a major advance in cancer therapy (41, 42). However, many Gleevec patients acquire resistance mutations to the drug or acquisition of Bcr-Abl–independent genetic abnormalities during the course of treatment (43–46). Thus, development of additional therapeutic approaches for CML and other malignancies is worthwhile. Here, we describe two sequence-specific DNA alkylators, 1R-Chl and 6R-Chl, which are capable of inhibiting K562 CML cell growth both *in vitro* and *in vivo*. 1R-Chl and 6R-Chl treatments are also highly effective in blocking K562 xenograft growth, with high-dose tolerance in the murine model. Based on these observations and the finding that 1R-Chl blocks SW620 xenograft growth in nude mice (32), and the growth of two other xenograft models (Calu-1 lung cancer cells and 22Rv1 prostate cancer cells; data not shown), polyamide-chlorambucil conjugates seem to be promising cancer therapeutics. The inhibitory mechanism of 1R-Chl and 6R-Chl in K562 cells is likely to be independent of Bcr-Abl because no significant down-regulation of Bcr-Abl transcripts was observed in either Affymetrix GeneChip analysis or real-time qRT-PCR (data not shown). These results suggest that 1R-Chl maybe an effective treatment alternative for CML or may be useful in combination with Gleevec.

Acknowledgments

We thank the staff of The Scripps Research Institute Department of Animal Resources, and The Scripps Mass Spectrometry and DNA Microarray facilities for technical assistance.

References

1. Lee ST, Neelapu SS, Kwak LW. Therapeutic vaccine for lymphoma. Yonsei Med J 2007;48:1–10.

2. Hengstler JG, Bockamp EO, Hermes M, et al. Oncogene-blocking therapies: new insights from conditional mouse tumor models. Curr Cancer Drug Targets 2006;6:603–12.

3. Johnston SRD, Leary A. Lapatinib: a novel EGFR/HER2 tyrosine kinase inhibitor for cancer. Drugs Today 2006;42:441 – 53.

4. Ren RB. Modeling the dosage effect of oncogenes in leukemogenesis. Curr Opin Hematol 2004;11:25 – 34.

5. O'Mahony D, Bishop MR. Monoclonal antibody therapy. Front Biosci 2006;11:1620 – 35.

6. Reid A, Vidal L, Shaw H, de Bono J. Dual inhibition of ErbB1 (EGFR/HER1) and ErbB2 (HER2/neu). Eur J Cancer 2007;43:481 – 9.

7. O'Hare T, Corbin AS, Druker BJ. Targeted CML therapy: controlling drug resistance, seeking cure. Curr Opin Genet Dev 2006;16:92 – 9.

8. Schittenhelm MM, Shiraga S, Schroeder A, et al. Dasatinib (BMS-354825), a dual SRC/ABL kinase inhibitor, inhibits the kinase activity of wild-type, juxtamembrane, and activation loop mutant KIT isoforms associated with human malignancies. Cancer Res 2006;66:473 – 81.

9. Filippini C, Bisiach M, Tagliabue G, Dincalci M, Ubezio P. Hematopoietic toxicity and cell cycle perturbations induced by new DNA minor groove-alkylating agents. Int J Cancer 1997;72:801 – 9.

10. Izbicka E, Tolcher AW. Development of novel alkylating drugs as anticancer agents. Curr Opin Investig Drugs 2004;5:587 – 91.

11. Neidle S, Thurston DE. Chemical approaches to the discovery and development of cancer therapies. Nat Rev Cancer 2005;5:285 – 96.

12. Weiss GR, Poggesi I, Rocchetti M, et al. A phase I and pharmacokinetic study of tallimustine [PNU152241 (FCE 24517)] in patients with advanced cancer. Clin Cancer Res 1998;4:53 – 9.

13. Lockhart AC, Howard M, Hande KR, et al. A phase I dose-escalation and pharmacokinetic study of brostallicin (PNU-166196A), a novel DNA minor groove binder, in adult patients with advanced solid tumors. Clin Cancer Res 2004;10:468 – 75.

14. Broggini M, Coley HM, Mongelli N, et al. DNA sequence-specific adenine alkylation by the novel antitumor drug tallimustine (Fce-24517), a benzoyl nitrogen-mustard derivative of distamycin. Nucleic Acids Res 1995;23:81 – 7.

15. Broggini M, Marchini S, Fontana E, Moneta D, Fowst C, Geroni C. Brostallicin: a new concept in minor groove DNA binder development. Anticancer Drugs 2004;15:1 – 6.

16. Herzig MCS, Trevino AV, Arnett B, Woynarowski JM. Tallimustine lesions in cellular DNA are AT sequence-specific but not region-specific. Biochemistry 1999;38:14045 – 55.

17. Dervan PB, Edelson BS. Recognition of the DNA minor groove by pyrrole-imidazole polyamides. Curr Opin Struct Biol 2003;13:284 – 99.

18. Dudouet B, Burnett R, Dickinson LA, et al. Accessibility of nuclear chromatin by DNA binding polyamides. Chem Biol 2003;10:859 – 67.

19. Best TP, Edelson BS, Nickols NG, Dervan PB. Nuclear localization of pyrrole-imidazole polyamide-fluorescein conjugates in cell culture. Proc Natl Acad Sci U S A 2003;100:12063 – 8.

20. Edelson BS, Best TP, Olenyuk B, et al. Influence of structural variation on nuclear localization of DNA-binding polyamide-fluorophore conjugates. Nucleic Acids Res 2004;32:2802 – 18.

21. Nickols NG, Jacobs CS, Farkas ME, Dervan PB. Improved nuclear localization of DNA-binding polyamides. Nucleic Acids Res 2007;35:363 – 70.

22. Dickinson LA, Gulizia RJ, Trauger JW, et al. Inhibition of RNA polymerase II transcription in human cells by synthetic DNA-binding ligands. Proc Natl Acad Sci U S A 1998;95:12890 – 5.

23. Olenyuk BZ, Zhang GJ, Klco JM, Nickols NG, Kaelin WG, Dervan PB. Inhibition of vascular endothelial growth factor with a sequence-specific hypoxia response element antagonist. Proc Natl Acad Sci U S A 2004;101:16768 – 73.

24. Nickols NG, Dervan PB. Suppression of androgen receptor-mediated gene expression by a sequence-specific DNA-binding polyamide. Proc Natl Acad Sci U S A 2007;104:10418 – 23.

25. Nickols NG, Jacobs CS, Farkas ME, Dervan PB. Modulating hypoxia-inducible transcription by disrupting the HIF-1-DNA interface. ACS Chem Biol 2007;2:561 – 71.

26. Janssen S, Cuvier O, Muller M, Laemmli UK. Specific gain- and loss-of-function phenotypes induced by satellite-specific DNA-binding drugs fed to *Drosophila melanogaster*. Mol Cell 2000;6:1013 – 24.

27. Janssen S, Durussel T, Laemmli UK. Chromatin opening of DNA satellites by targeted sequence-specific drugs. Mol Cell 2000;6:999 – 1011.

28. Burnett R, Melander C, Puckett JW, et al. DNA sequence-specific polyamides alleviate transcription inhibition associated with long GAA center dot TTC repeats in Friedreich's ataxia. Proc Natl Acad Sci U S A 2006;103:11497 – 502.

29. Wurtz NR, Dervan PB. Sequence specific alkylation of DNA by hairpin pyrrole-imidazole polyamide conjugates. Chem Biol 2000;7:153 – 61.

30. Oyoshi T, Kawakami W, Narita A, Bando T, Sugiyama H. Inhibition of transcription at a coding sequence by alkylating polyamide. J Am Chem Soc 2003;125:4752 – 4.

31. Shinohara K, Narita A, Oyoshi T, Bando T, Teraoka H, Sugiyama H. Sequence-specific gene silencing in mammalian cells by alkylating pyrrole-imidazole polyamides. J Am Chem Soc 2004;126:5113 – 8.

32. Dickinson LA, Burnett R, Melander C, et al. Arresting cancer proliferation by small-molecule gene regulation. Chem Biol 2004;11:1583 – 94.

33. Tsai SM, Farkas ME, Chou CJ, Gottesfeld JM, Dervan PB. Unanticipated differences between α- and γ-diaminobutyric acid-linked hairpin polyamide-alkylator conjugates. Nucleic Acids Res 2007;35:307 – 16.

34. Farkas ME, Tsai SM, Dervan PB. α-Diaminobutyric acid-linked hairpin polyamides. Bioorg Med Chem 2007;15:6927 – 36.

35. Alvarez D, Chou CJ, Latella L, et al. A two-hit mechanism for premitotic arrest of cancer cell proliferation by a polyamide-alkylator conjugate. Cell Cycle 2006;5:1537 – 48.

36. Baird EE, Dervan PB. Solid phase synthesis of polyamides containing imidazole and pyrrole amino acids. J Am Chem Soc 1996;118:6141 – 6.

37. Trauger JW, Dervan PB. Footprinting methods for analysis of pyrrole-imidazole polyamide/DNA complexes. Methods Enzymol 2001;340:450 – 66.

38. Garrity PA, Wold BJ. Effects of different DNA-polymerases in ligation-mediated PCR: enhanced genomic sequencing and *in vivo* footprinting. Proc Natl Acad Sci U S A 1992;89:1021 – 5.

39. Sabatino MA, Colombo T, Geroni C, Marchini S, Broggini M. Enhancement of *in vivo* antitumor activity of classical anticancer agents by combination with the new, glutathione-interacting DNA minor groove-binder, brostallicin. Clin Cancer Res 2003;9:5402 – 8.

40. Shinohara K, Sasaki S, Minoshima M, Bando T, Sugiyama H. Alkylation of template strand of coding region causes effective gene silencing. Nucleic Acids Res 2006;34:1189 – 95.

41. Druker BJ, Sawyers CL, Kantarjian H, et al. Activity of a specific inhibitor of the BCR-ABL tyrosine kinase in the blast crisis of chronic myeloid leukemia and acute lymphoblastic leukemia with the Philadelphia chromosome. N Engl J Med 2001;344:1038 – 42.

42. Druker BJ, Talpaz M, Resta DJ, et al. Efficacy and safety of a specific inhibitor of the BCR-ABL tyrosine kinase in chronic myeloid leukemia. N Engl J Med 2001;344:1031 – 7.

43. Jahagirdar BN, Miller JS, Shet A, Verfaillie CM. Novel therapies for chronic myelogenous leukemia. Exp Hematol 2001;29:543 – 56.

44. Capdeville R, Buchdunger E, Zimmermann J, Matter A. Glivec (ST1571, imatinib), a rationally developed, targeted anticancer drug. Nat Rev Drug Discov 2002;1:493 – 502.

45. von Bubnoff N, Peschel C, Duyster J. Resistance of Philadelphia-chromosome positive leukemia towards the kinase inhibitor imatinib (STI571, Glivec): a targeted oncoprotein strikes back. Leukemia 2003;17:829 – 38.

46. Nimmanapalli R, Bhalla K. Mechanisms of resistance to imatinib mesylate in Bcr-Abl-positive leukemias. Curr Opin Oncol 2002;14:616 – 20.